SCIENCE CHINA
Chemistry

• REVIEWS •
· SPECIAL TOPIC · Single-Molecule, Single-Particle and Single-Cell Bioimaging

October 2017 Vol.60 No.10: 1267–1276
doi: 10.1007/s11426-017-9097-4

Recent advances in optical-based and force-based single nucleic acid imaging

Shenshan Zhan[1], Xiaoding Lou[1,2] & Fan Xia[1,2,3*]

[1]*Hubei Key Laboratory of Bioinorganic Chemistry & Materia Medica, School of Chemistry and Chemical Engineering, Huazhong University of Science and Technology, Wuhan 430074, China*
[2]*Faculty of Material Science and Chemistry, China University of Geosciences, Wuhan 430074, China*
[3]*Shenzhen Institute of Huazhong University of Science and Technology, Shenzhen 518000, China*

Received April 20, 2017; accepted June 14, 2017; published online August 11, 2017

The capability to image, as well as control and manipulate single molecules such as nucleic acids (DNA or RNA) can greatly enrich our knowledge of the roles of individual biomolecules in cellular processes and their behavior in native environments. Here we summarize the recent advances of single nucleic acid imaging based on optical observation and force manipulation. We start by discussing the superiority of single molecule image, the central roles nucleic acids play in biosystems, and the significance of single molecule image towards nucleic acids. We then list a series of representative examples in brief to illustrate how nucleic acid of various morphologies has been imaged from different aspects, and what can be learned from such characterizations. Finally, concluding remarks on parts of which should be improved and outlook are outlined.

single nucleic acid imaging, optical-based observation, force-based manipulation, fluorescent imaging, atomic force microscopy

Citation: Zhan S, Lou X, Xia F. Recent advances in optical-based and force-based single nucleic acid imaging. *Sci China Chem*, 2017, 60: 1267–1276, doi: 10.1007/s11426-017-9097-4

1 Introduction

Observation, as well as manipulation and control of individual molecules can greatly deepen our understanding on the structure-functional-mechanical working of molecular machinery [1]. Since the observation of single molecules and atoms in real space has been achieved by atomic force microscopy (AFM) [2] and scanning tunneling microscopy (STM) [3], technologies for imaging and manipulation of individual molecules such as growth factors, proteins and nucleic acids have been emerged continuously in the past thirty years [4–9]. Most spectroscopic technologies that depend on the production of a strong signal by a large ensemble of molecules are useful as they enable the measurement by raising the signal above the noise, but limits remain that a great quantity of sample are required and only ensemble-averaged information could be provided [10,11]. On the contrary, in a single molecule experiment, the inhomogenous distributions of diverse origins that perplex the measurements on large ensembles are avoided and the usual averaging over large populations is eliminated [12], direct access to the mean values and the higher order moments of the kinetic coefficients that characterize a nonuniform kinetic behavior, dynamic process as well as transient, rare or unlikely molecular states can be provided, and complex spatiotemporal distributions with properties of ensembles of individual molecules in an single specimen or cell can also be revealed [13].

*Corresponding author (email: xiafan@hust.edu.cn)

In the past several decades, single molecule imaging technologies have made significant progresses in applications such as bioassay chips and fundamental molecular mechanism studies, among which imaging of nucleic acids (NAs: DNA or RNA) is one of the most indispensable areas due to the important roles NAs play in biosystems including transcription, translation, catalysis and regulation of gene expression [14–16]. The early studies of single NA imaging can be tracked to 1980s. Morikawa *et al*. [17] and Houseal *et al*. [18] respectively developed an optical microscopy technique to visualize the dynamics of individual DNA molecules free in solution. By depositing uncoated DNA that dissolved in salt solution on graphite and imaging them in air with the STM, Beebe *et al*. [19] and Keller *et al*. [20] obtained the high-resolution images of single DNA. Since it reveals new insights into the physical and biological properties of NAs, and helps us to explore the genetic characterization of each molecule, construct genome map and identify abnormal genes, imaging of NAs at the single molecule level becomes more and more attractive [14,15]. While there have been plentiful detailed technical reports and expert review articles on the design, fabrication and application of single molecule imaging techniques [21–23], this review mainly focus on examples of single NA imaging in recent five years (2013–2017).

2 Single nucleic acid imaging

Most single molecule imaging techniques generally fall into two categories [24,25]: optical-based observation via fluorescence or plasmonics [26] and force-based manipulation such as AFM, flow stretching, optical tweezers and magnetic tweezers [27]. While experiments of the first category allow localizing and distinguishing molecular species and tracking unconstrained molecular behavior, in the second category mechanical stimuli are applied to probe mechanical properties or to regulate kinetic processes [28].

2.1 Optical-based single nucleic acid imaging

2.1.1 Fluorescence-based imaging

For single NA imaging, structure and dynamics are usually the two main topics [29], of which the later were often carried out based on the former's researches. By utilizing the intrinsic invertible photo-blinking of DNA binding dye, Miller *et al*. [30] reconstructed the details of the molecular structure of individual DNA molecules *in vitro* with a localization precision which is less precise by almost an order of magnitude in a diffraction-limited regime than the standard optical resolution limit, both for the intercalating dye YOYO-1 (Figure 1(a)) and the minor groove binding dye SYTO-13 (Figure 1(b)). The localization precision observed of several tens of nanometers (nm) could be increased by shortening the time resolution of sampling in principle, at the expense of weakening the capacity to resolve surrounding fluorophores. The system's ability to capture super-resolved images at video-rate sampling indicates its broad prospects for real-time observation of dynamic topology of DNA [30].

When study the dynamics of NA, single molecule orientation measurement was prior used as it provide unprecedented insight into multitudes of biological and polymeric systems. By combining polarization modulation with localization microscopy, Backer *et al*. [31] reported a simple, high-throughput technique for measuring single molecule rotational dynamics, detecting nanoscale deformations in individual DNA strands, and characterizing the binding modes of different types of DNA staining dyes (Figure 2). Using their method, the prevalence and severity of such orientation-induced errors could be ascertained, and appropriate correction schemes could be implemented when necessary, thus a wide range of single molecule imaging experiments would benefit from this method [32].

Though the science and technology has enter the era in which super-resolution image as precise as single molecule could be realized, a variety of large scale and expensive equipment were essentially demanded, which on some extent restrict the wider employment and deeper development of these technologies. Over the past decade, mobile phones with smaller sizes and smarter functions were emerged in large numbers day by day, based on which researchers throughout the world have creatively designed a variety of microscopy and sensing platforms for point of care testing (POCT) [33].

Wei *et al*. [34] demonstrated the first example of visualization and measurement of individual DNA molecules on a mobile phone microscope. This simple, cost-effective, and field-portable fluorescent microscopy platform assembled on a mobile phone permits direct observation of individual fluorescently-labeled DNA molecules over a wide field-of-view (FOV) with ~2 mm^2. A robust image processing framework that is integrated with the cloud was also developed to overcome the signal-to-noise ratio (SNR) challenge as well as allow quantitative length measurements of single DNA molecules observed on the mobile phone platform, achieving a sizing accuracy of <1000 base pair (bp) for 10000 bp and longer DNA samples (Figure 3). This mobile phone based imaging platform provides a unique solution for sizing DNA molecules and might also be utilized for determining copy number variations (CNVs) in genome, thus possessing a distinct capability that can be potentially used in various clinical applications including for the detection of cancers, nervous system disorders or even drug resistance in infectious diseases. Through offering spatiotemporal data mapping, this platform could also assist, e.g., epidemiologists, health-care professional and policy makers, to track emerging trends and shed more light on genetic cause-effect relationships in POCT and resource limited settings [34]. Recently, a new

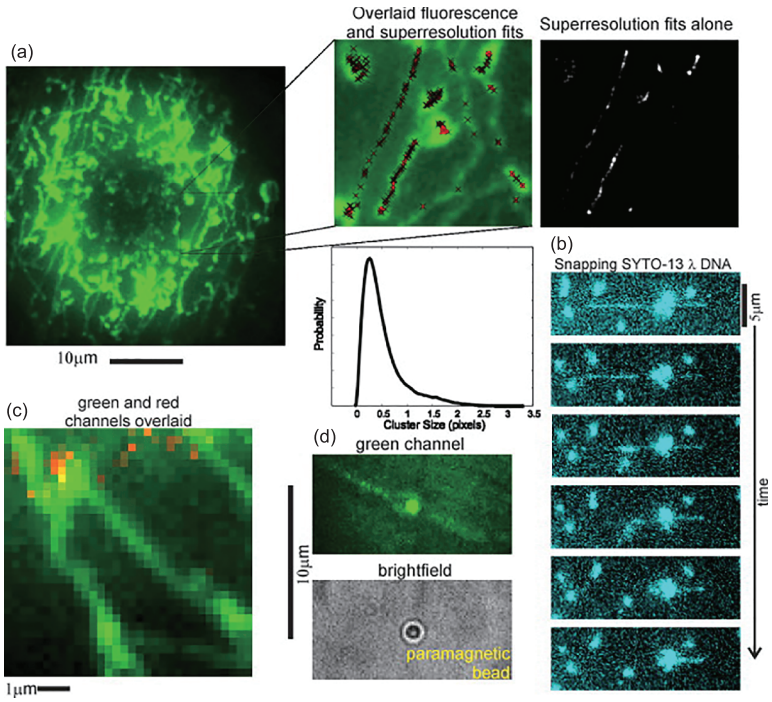

Figure 1 (a) Fluorescence imaging of YOYO-1 labeled lambda phage DNA (λ-DNA) (green). The ADEMS code reconstruction in red and clusters as black crosses are shown in left panel, and the compiled super-resolution fits alone are shown in right panel of the expanded section. The cluster size distribution of position from ADEMS code is also shown. (b) Continuous micrograph images of SYTO-13 labeled λ-DNA that firstly combed straight and then snapped back following prolonged laser excitation. (c) Overlaid red channel (digoxigenin terminus of DNA construct) and green channel (DNA). (d) Green channel and bright-field frames of a paramagnetic bead linked to two fluorescently labeled DNA strands. Note: the ADEMS code is a home written program designed by the authors. Reprinted with permission from Ref. [30]. Copyright (2015) Elsevier Ltd. (color online).

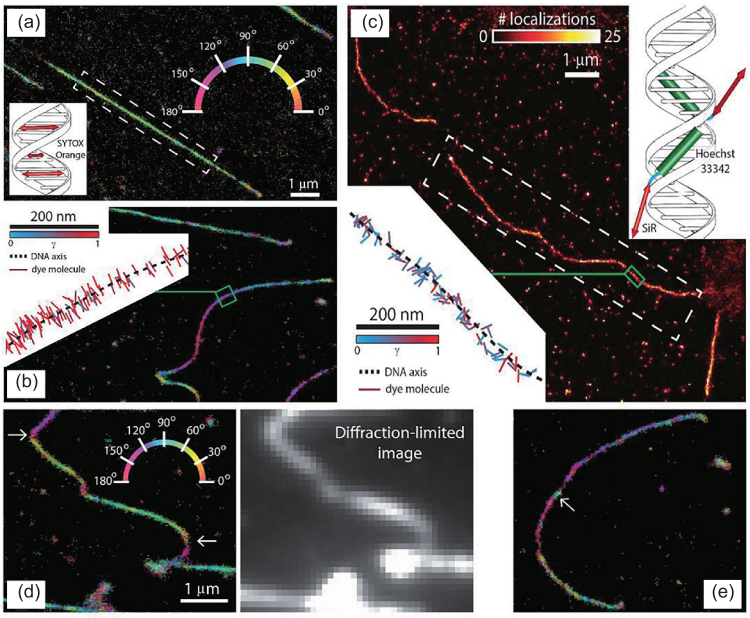

Figure 2 (a) Images of λ-DNA strands which are color coded in accordance with the mean azimuthal orientation of dye molecules monitored within 30 nm voxels. Inset: absorbtion dipole moments align perpendicular to the DNA axis as a result of the intercalative binding mode. (b) A bended DNA strand of which the mean molecular orientation rotates to keep perpendicular to the DNA axis. Inset: visualization of all orientation measurements localized along a short fragment of DNA (green box). (c) An ultra-resolution image of a DNA strand. As the silicon-rhodamine (SiR) is not bound to DNA strands directly, the absorbtion dipole moments of it are not constrained (right inset). This feature is confirmed by the visualization of all orientation measurements localized within a small fragment of DNA (green boxed region and lower left inset). (d) A super-resolved image of a λ-DNA strand possessing multiple "bends". A diffraction-limited image was generated by summing all frames of data included in the acquisition sequence for comparison. (e) A super-resolved image of a λ-DNA strand showing "tangles". Note: SYTOX Orange was used in (a), (b), (d) and (e), and SiR-Hoechst was used in (c). Adapted with permission from Ref. [31]. Copyright (2016) The Optical Society (color online).

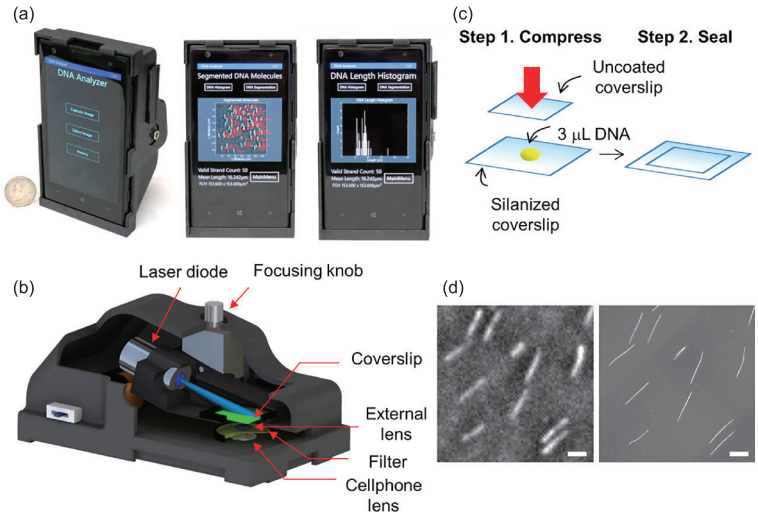

Figure 3 Visualization and measurement of single DNA molecules on a mobile phone. (a) Photographs of the mobile phone based fluorescence microscopy. (b) Illustration of the same optomechanical attachment. (c) Illustration of a simple DNA stretching method used in this work. (d) Typical fluorescence microscope frames of uncoiled λ-DNA molecules that obtained by using (left) the mobile phone microscope and (right) a benchtop fluorescence microscope (oil-immersion objective lens=100×, numerical aperture=1.3). Scale bar: 10 μm. Reprinted with permission from Ref. [34]. Copyright (2014) American Chemical Society (color online).

milestone for tele-medicine technologies was achieved by the same group. They developed another molecular assay and hand-held optical imaging device that allows POCT with a cost-efficient mobile phone based multi-modal microscope [35]. By using this mobile phone microscopy, *in-situ* detection of the point mutation assays in preserved tumor samples and targeted next-generation DNA sequencing reactions were analyzed and imaged.

2.1.2 Plasmonic-based imaging

Fluorescence imaging has revolutionized the biological research [36]. However, the requirement for tedious sample preparation probably distort the native properties of the molecules, and the relatively slow imaging speed and weak fluorescence emission, blinking and photo-bleaching make it not suitable for fast imaging or quantifying the image intensity or studying individual molecules for a long time [37–39], thus substitute methods for single molecule imaging have been established by researchers.

Yu *et al*. [38] reported the first label-free differential surface plasmon resonance (DSPR) technique for imaging of individual DNA molecules. Plasmons were excited optically at a gold film surface, on which the DNA molecules scattered the related propagating plasmonic waves and generated a unique plasmonic image with contrast several orders of magnitude clearer than the image of traditional bright field optical microscopy. Through changing the propagation direction of the plasmonic wave proportional to the orientation of the DNA strands that extended on the surface, the image contrast was studied and the DSPR images with theoretical simulation and fluorescence images were compared (Figure 4). To further strengthen the image contrast and realize single

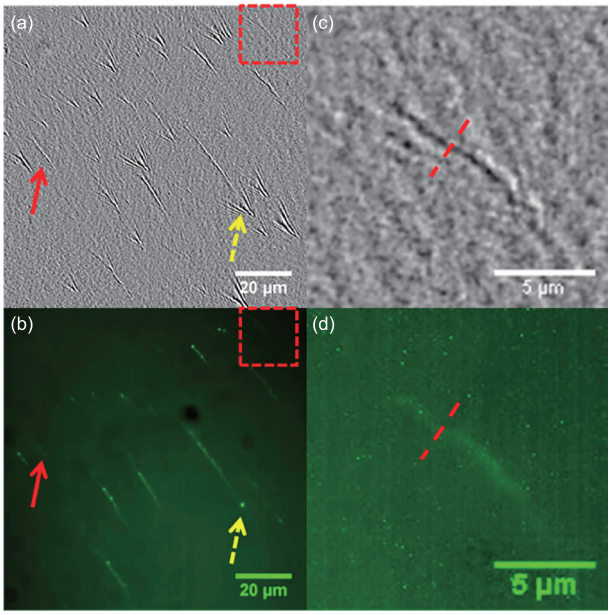

Figure 4 (a, b) Representative DSPR and fluorescence images of the stretched λ-DNA deposited on gold surface; (c, d) zoomed-in images of individual DNA molecule in the dotted boxes in (a) and (b). Reprinted with permission from Ref. [38]. Copyright (2014) American Chemical Society (color online).

DNA molecules imaging, needless interference patterns and noises arise from the optical system were eliminated with the differential method. The characteristics of label-free, rapid, and quantitative enable this method suited for single molecule DNA analysis.

2.2 Force-based single nucleic acid imaging

Whereas there is an ever expanding report of single molecule

manipulation techniques [40], including AFM [41], flow induced stretching [42], optical tweezers [43–45], magnetic tweezers [46–48], micro-needle manipulation [49], and biomembrane force probe [50], the first three have been employed in single NA imaging in recent five years and are the focus of this section.

2.2.1 AFM-based imaging

Several characteristics of NA, such as uniform dimensions, relatively nonconducting nature, and easy physical identification of ~2 nm wide filamentous feature, predispose NA to being probed by AFM [51].

AFM stands out as one of the most attractive technique to image the interaction between an individual DNA molecule and its ligands because of its ability to observing DNA strands with sub-nm resolution or to characterizing their mechanical behaviors on a single molecule level [52,53]. Alonso-Sarduy *et al*. [54] presented an AFM characterization of the impact of daunorubicin and ethidium bromide on DNA in physiological medium for the first time. Conformational transitions resulted from the exposure to daunorubicin within the varying topological structures of DNA were monitored (Figure 5), and the results were compared with the ones obtained using ethidium bromide. Additionally, the intercalating-agents-induced transitions in time-lapse were followed, and the consequent modification in the DNA super-coiling and characterization of the interactions that was unheard-of for its spatial-temporal resolution were also delivered. These findings were excellently coincide with the existing reports that investigated DNA in solution [55], paving the way for a deeper characterization of these transitions, and shedding more light on the still deficiently studied field of interactions between DNA and drugs [56].

As the genetic material of various viruses, the double-stranded RNA (dsRNA) has been acknowledged as a related molecule in cells because of its regulatory effect for almost 20 years [57–59]. However, its elastic response has not been characterized in single molecule experiments equivalently like that of double-stranded DNA (dsDNA) [60–62]. By applying optical tweezers, magnetic tweezers and AFM, Moreno-Herrero's group [63] monitored the individual characteristics of the long dsRNA molecules, and compared the results with the behaviour of dsDNA molecules which possess the identical sequence (Figure 6). Results show that unlike in physiological conditions, dsRNA does not transform from the A- to B-form in the present of force, and it exhibits both an overstretching transition force and lower stretch modulus than dsDNA, with larger intrinsic and electrostatic contributions to the persistence length [63].

Combining soft-touch AFM with image analysis and without needing crystallization, Pyne *et al*. [64] described a strategy to reproduce the secondary structure of single plasmid (Figure 7). The method was verified by precisely reconstructing the appearance of the B-DNA crystal structure. Especially, intra-molecular changes in groove deepness of the DNA double helix that was unprocurable for methods depend on ensemble-averaging was also resolved. In 2016 the same group reported the images of individual dsRNA molecules with sub-helical resolution obtained with AFM [65]. Both the minor and major grooves were resolved and the helical pitch utilizing different force and dynamic-based imaging modes was quantified, with the result of 3.1±0.3 nm that consistent with the A-form of dsRNA. Results acquired from three different imaging modes (i.e., amplitude modulation,

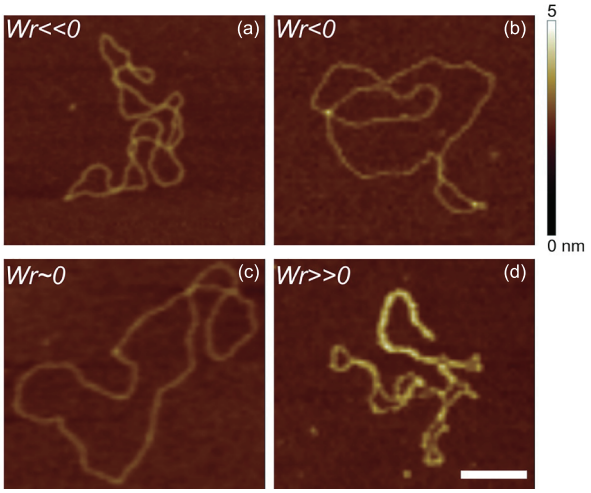

Figure 5 Typical topographic AFM images of DNA molecules stained with daunorubicin of different concentrations. (a) 0; (b) 2.5 μM; (c) 10 μM; (d) 40 μM. Scale bar: 100 nm. The top left corner of each image showed the approximate writhe that each molecule possessed. The surface height was indicated by the color scale common to all four images. Reprinted with permission from Ref. [54]. Copyright (2013) American Chemical Society (color online).

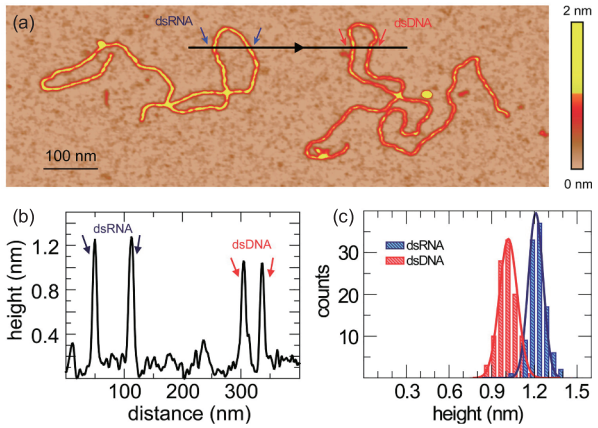

Figure 6 (a) AFM images of two characteristic dsRNA and dsDNA precipitated on a same surface. Color scale (0–2 nm) was regulated to give prominence to the measured height of dsRNA. (b) Height profile of the dsRNA and dsDNA molecules adopted in the direction of the black arrow shown in (a). (c) Height distribution of dsRNA and dsDNA molecules adsorbed over the same surface. Reprinted with permission from [63]. Copyright (2013) American Chemical Society (color online).

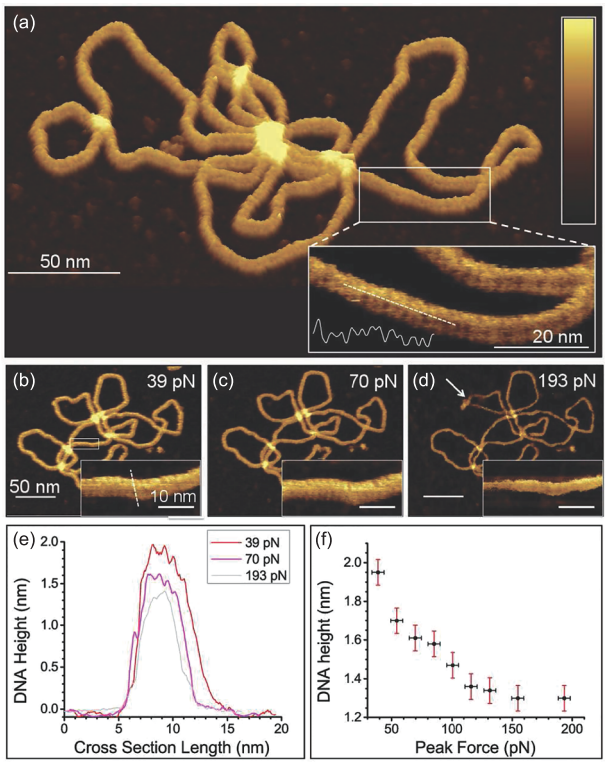

Figure 7 (a–d) AFM images of a plasmid exhibiting the integrated appearance of the DNA helix obtained with different peak forces. Insets: minor and major grooves observed scanned in AFM images. (e) Height profiles measured across the DNA for varying peak forces as depicted on the inset of (b) by a dotted line. (f) Measured height as a function of peak force along the same section across the molecule. White arrow denotes a dislocation in a plasmid loop produced by high load forces. Reprinted with permission from Ref. [64]. Copyright (2014) John Wiley & Sons (color online).

AM; drive amplitude modulation, DAM and jumping mode plus, JM+) shown parallel resolution under optimal operating conditions (Figure 8). By simulating these AFM images, it was found that radius as short as 2.5 nm is required to differentiate both the minor and major grooves. This finding provides powerful evidence that, instead of the imaging pattern, the sharpness of the AFM tip apex and the force between tip and sample are crucial for acquiring high resolution [66].

2.2.2 Flow stretching-based imaging

From the above-mentioned examples of AFM-based single NA imaging, it could be seen that those NAs were exhibited in random coil status, of which the full length could not be clearly revealed. In order to circumvent this problem, another commonly used force-based imaging method, flow stretching-based imaging was employed [67,68].

Neupane *et al.* [69] demonstrated a facile DNA stretching strategy which could stretch DNA to its full length and both fit for fluorescent and AFM imaging (Figure 9). Two competing forces on the DNA molecules, i.e., the centrifugal force of the rotating substrate, and the electrostatic attraction between the negatively charged surface of glass substrate and the positively charged YOYO-1 that intercalated into DNA, were primarily accountable for the efficient dispersion and stretching of the single DNA strands. The density of the stretched DNA molecules could be regulated by varying the solution concentration of the dye-stained DNA. Since the photoluminescence spectra of individual DNA molecule dyed with YOYO-1 were acquired and the stretching of individual DNA molecules was identified by AFM imaging, it is

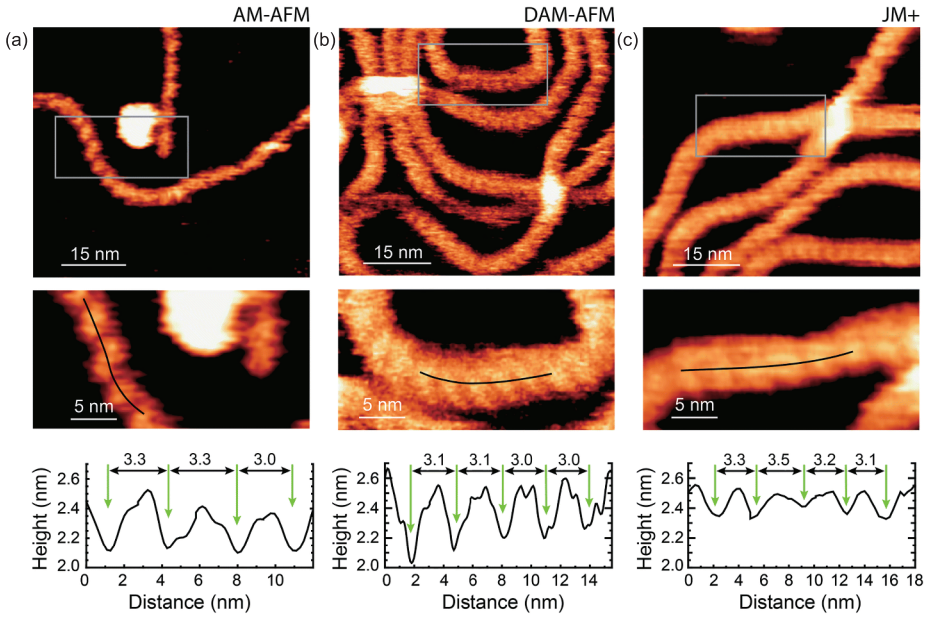

Figure 8 AFM images of dsRNA obtained with the (a) AM-AFM, (b) DAM-AFM, and (c) JM+ imaging modes. Top row: wide FOV containing several dsRNA molecules; Middle row: details at higher magnification of the squared region marked in the top row; Bottom row: height profiles along the lines depicted in the zoomed-in images. The corrugation observed along the dsRNA was highlighted by regulating the color scale. Reprinted with permission from Ref. [65]. Copyright (2016) Royal Society of Chemistry (color online).

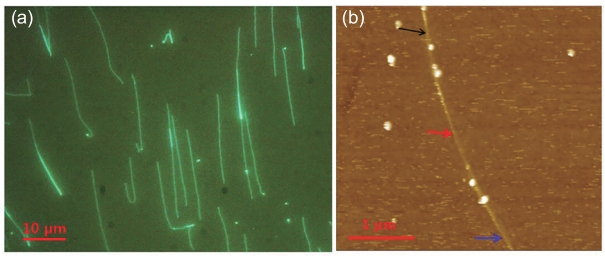

Figure 9 (a) Fluorescence images of stretched λ-DNA molecules acquired with DNA-dye solutions (concentration: 7.5 ng/μL); (b) AFM image of stretched λ-DNA molecule dyed with YOYO-1. Adapted with permission from Ref. [69]. Copyright (2014) The SPIE Publications (color online).

suggested that this method was practical for spectroanalysis of DNA at the single molecule level [69].

By integrating dynamic molecular combing (DMC) and stimulated emission depletion (STED) nanoscopy, Kim *et al*. [70] measured the length of single DNA segments that stretched on a coverslip linearly (Figure 10). Without no elaborate covalent conjugation steps, *Hin*dIII- and *Bst*EII-treated λ-DNA fragments were simply mixed with YOYO-1 and then stretched on a coverslip by DMC. The image of single DNA segments was acquired by STED nanoscopy. By using this strategy, the lengths of DNA segments ranging extensively in size (117–23130 bp) could be precisely and accurately measured by super-resolved imaging. The measured lengths of the DNA segments were coincidentally within 0.5% to 1.0% of the reference values when the DNA segments were longer than ~1000 bp, revealing the potential of this strategy in an extensive range of utilization including convenient detection for trinucleotide repeat disorder and CNVs [70].

In order to avoid the manual manipulation of individual DNA molecules, Sørensen *et al*. automated the critical steps of the operation of a nanofluidic device for stretching and imaging megabase-long DNA molecules based on real-time fluorescence images analysis (Figure 11). By applying pressure driven flows, single molecules were picked from a microchannel and stretched with picoNewton (pN) forces. The image analysis for machine vision were challenged as the DNA segments of millimeter-long freely flowed in micro/nanofluidics emitting weak fluorescence and changing shape. Besides a series of image-processing steps that raise the intrinsically low SNR linked with single molecule fluorescence microscopy, estimation of the molecules length by sequential real-time image stitching and improvement of the resolution efficiency of a pressure controller by pulse width modulation were also demonstrated. In particular, solution for using imaging of genomic DNA molecules as feedback for automation was also reported, despite the fact that both the shape and intensity of individual molecules change due to the hydrodynamic shearing in a micro and nanofluidic environment [71]. This device represents a step toward improving the throughput of the unique platform for imaging fluorescence barcodes on megabase-long DNA [72].

2.2.3 Optical tweezer-based imaging

Since the optical tweezers can provide sub-nm resolution in length scales and sub-pN resolution for force, and have been widely employed to investigate the melting transition of single DNA molecules as well as the interaction between DNA and proteins or drugs in real-time [73,74], they are also well suitable to research the mechanical properties of biomolecules such as DNA [44].

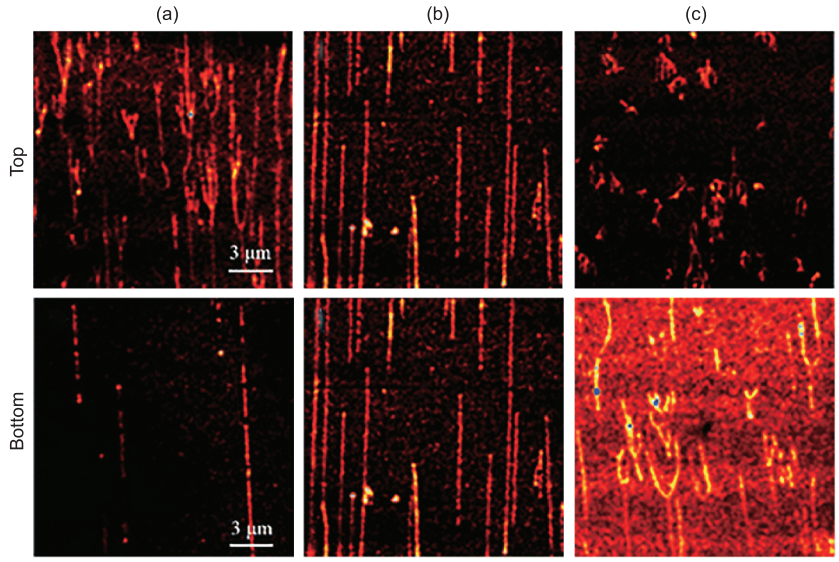

Figure 10 Top: Images of the combed λ-DNAs of different linearity applying pull-up speeds of (a) 20 μm/s, (b) 200 μm/s, and (c) 1000 μm/s. Bottom: images of the combed λ-DNAs of different brightness utilizing ratios of (a) 1:30, (b) 1:5, and (c) 1:1 of dye per bp in the buffer. Reprinted with permission from Ref. [70]. Copyright (2016) Springer-Verlag Berlin Heidelberg (color online).

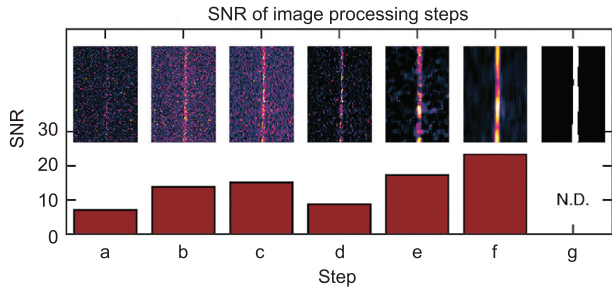

Figure 11 Image processing steps for machine vision of sheared DNA. (a) Raw image of a single DNA strand in the nanoslit. Same strand after (b) frame averaging, (c) parallel binning, (d) background subtraction, (e) median filtering, and (f) anisotropic filtering to emphasize long objects. (g) Binary image used for machine vision. The SNR of each step is shown except for (g) as the background variance is zero. Reprinted with permission from Ref. [71]. Copyright (2015) The AIP Publishing (color online).

With the help of optical tweezers, Suei *et al*. [75] studied the covalent attachment of fluorescent dyes (6-carboxyfluorescein (6-FAM) or Eterneon) to dsDNA stretched between particles, and compared the mechanical properties of the covalently modified chain with that of the DNA bound to SYBR-gold and the unmodified one (Figure 12). Modified DNA was acquired by linking azide-functionalized 6-FAM or Eterneon onto the DNA backbone via the alkyne moieties that had been integrated into modified bases during polymerase chain reaction (PCR). Then these modified DNA molecules were fabricated into dumbbells by jointing polystyrene (PS) particles to the respective chain terminals via digoxigenin or biotin handles that had been pre-integrated into the PCR primers. Subsequently, the DNA was extended by drawing away the two optically trapped PS particles using the optical tweezers. By applying an interpolation-based normalized cross-correlation method, the displacements of the PS particles were measured in 3D. The DNA mechanical properties were parameterized by calculating and fitting the force-extension curves into a worm-like chain model. Results showed the contour length of the strand was affected by the SYBR-gold binding in a force-dependent manner, whereas both the persistence and contour lengths of the covalently functionalized dsDNAs were undistinguishable from that of the unmodified one [75].

3 Conclusions

This review summarized the main advances of the single nucleic acid (NA: DNA or RNA) imaging in recent five years by dividing the techniques used into two broad categories: optical-based observation and force-based manipulation. By applying single molecule techniques of these two categories, single NA of different morphologies, either in random coil status or has been stretched to full length, as well as different aspects of single NA, from structure to dynamics, have been

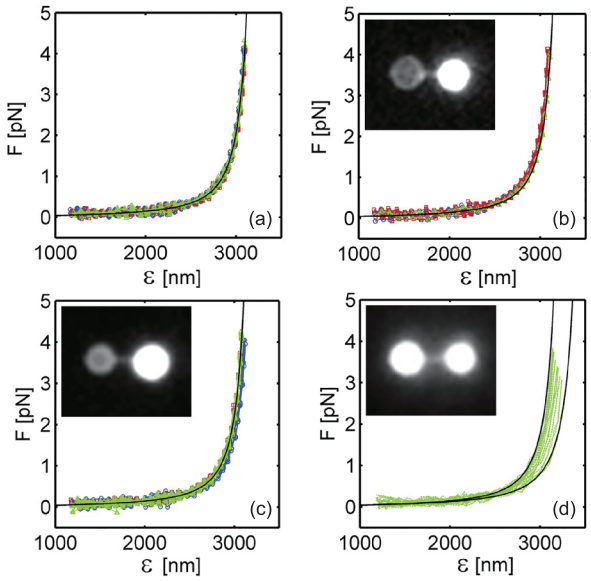

Figure 12 Data acquired from (a) three measurements performed on original DNA controls, (b, c) three measurements of 6-FAM and Eterneon labeled DNA, and (d) a set of 13 stretches of a DNA chain stained with SYBR-gold, accompany with a typical fit in each situation. Insets show the visualized individual DNA. Reprinted with permission from Ref. [75]. Copyright (2015) Elsevier Ltd. (color online).

revealed in super resolution. Thanks to these advances, researchers obtained deeper understanding of the structure-functional-mechanical working of NAs.

Despite the progress made, there is ample room, and indeed need, for single molecule techniques to further probe into the mechanisms of NA at the single molecule level. Firstly, from the aforesaid examples, it could be seen that fluorescent image and AFM are still the prevailing techniques, and except in one or two cases, most techniques were applied in isolation. Thus in the subsequent study, more new techniques and combined methods are highly encouraged. It is anticipated that new hybrid instruments that combine single molecule optics and force microscopy carry great potential for simultaneously observing multiple aspects of NAs dynamics [1,76], and will provide excellent sensitivity, prominent spatial resolution and remarkable penetration depth in a single system, greatly improve the quality of imaging [77]. Secondly, potentials of these existing techniques have not been explored adequately. Taken fluorescent image as an example, besides fluorescence intensity-based tracking and localizations, *in-situ* individual molecule studies founded on molecular spectroscopic properties such as the fluorescence polarization, spectrum, and lifetime are hopeful to bring deeper understanding into the molecular mechanisms of NAs [24]. Last but not least, as NA is one of the fundamental materials of life, it is predictable that dynamic imaging will be more attractive than static imaging and that is on which more effort should be put. Take the example of genetic analysis, as it has become increasingly evident that structural variation of NA plays an significant role

in common diseases and human health [78], it is reasonable to believe that imaging these variations dynamically at single molecule level may secure more time for promoting early detection, diagnosis and treatment of the diseases and even offer greater probability of keeping those related diseases far away.

Acknowledgments This work was supported by the National Natural Science Foundation of China (21525523, 21574048, 21375042, 21405054), the National Basic Research Program of China (2015CB932600, 2013CB933000), the Special Fund for Strategic New Industry Development of Shenzhen, China (JCYJ20150616144425376), and 1000 Young Talent (to Fan Xia).

Conflict of interest The authors declare that they have no conflict of interest.

1 Cordova JC, Das DK, Manning HW, Lang MJ. *Curr Opin Struct Biol*, 2014, 28: 142–148
2 Binnig G, Quate CF, Gerber C. *Phys Rev Lett*, 1986, 56: 930–933
3 Binnig G, Rohrer H. *Rev Mod Phys*, 1987, 59: 615–625
4 Zhang M, He K, Wu J, Li N, Yuan J, Zhou W, Ye Z, Li Z, Xiao H, Lv Z, Zhang Y, Fang X. *Sci China Chem*, 2017, 275: doi: 10.1007/s11426-017-9072-5
5 Willets KA, Ostroverkhova O, He M, Twieg RJ, Moerner WE. *J Am Chem Soc*, 2003, 125: 1174–1175
6 Gordon MP, Ha T, Selvin PR. *Proc Natl Acad Sci USA*, 2004, 101: 6462–6465
7 Stroh C, Wang H, Bash R, Ashcroft B, Nelson J, Gruber H, Lohr D, Lindsay SM, Hinterdorfer P. *Proc Natl Acad Sci USA*, 2004, 101: 12503–12507
8 Rasnik I, McKinney SA, Ha T. *Nat Meth*, 2006, 3: 891–893
9 Finkelstein IJ, Visnapuu ML, Greene EC. *Nature*, 2010, 468: 983–987
10 Gu JY, Cai ZF, Wang D, Wan LJ. *ACS Nano*, 2016, 10: 8746–8750
11 Arroyo JO, Kukura P. *Nat Photon*, 2015, 10: 11–17
12 Moerner WE, Orrit M, Wild UP, Basché T. *Single-molecule Optical Detection, Imaging and Spectroscopy*. New York: John Wiley & Sons, 2008
13 Walter NG, Bustamante C. *Chem Rev*, 2014, 114: 3069–3071
14 Duzdevich D, Redding S, Greene EC. *Chem Rev*, 2014, 114: 3072–3086
15 Gan JH, Sheng J, Huang Z. *Sci China Chem*, 2011, 54: 3–23
16 Min X, Zhang M, Huang F, Lou X, Xia F. *ACS Appl Mater Interfaces*, 2016, 8: 8998–9003
17 Morikawa K, Yanagida M. *J Biochem*, 1981, 89: 693–696
18 Houseal TW, Bustamante C, Stump RF, Maestre MF. *BioPhys J*, 1989, 56: 507–516
19 Beebe TP, Wilson TE, Ogletree DF, Katz JE, Balhorn R, Salmeron MB, Siekhaus WJ. *Science*, 1989, 243: 370–372
20 Keller D, Bustamante C, Keller RW. *Proc Natl Acad Sci USA*, 1989, 86: 5356–5360
21 Veigel C, Schmidt CF. *Nat Rev Mol Cell Biol*, 2011, 12: 163–176
22 Finkelstein IJ, Greene EC. *DNA Recombination: Methods and Protocols*. Totowa: Humana Press, 2011. 447–461
23 Moerner WE. *Proc Natl Acad Sci USA*, 2007, 104: 12596–12602
24 Xia T, Li N, Fang X. *Annu Rev Phys Chem*, 2013, 64: 459–480
25 Hohng S, Lee S, Lee J, Jo MH. *Chem Soc Rev*, 2014, 43: 1007–1013
26 Kozankiewicz B, Orrit M. *Chem Soc Rev*, 2014, 43: 1029–1043
27 Bustamante C, Cheng W, Mejia YX, Meija YX. *Cell*, 2011, 144: 480–497
28 Kemmerich FE, Swoboda M, Kauert DJ, Grieb MS, Hahn S, Schwarz FW, Seidel R, Schlierf M. *Nano Lett*, 2016, 16: 381–386
29 Lyubchenko YL. *Cell Biochem Biophys*, 2004, 41: 075–098
30 Miller H, Zhou Z, Wollman AJM, Leake MC. *Methods*, 2015, 88: 81–88
31 Backer AS, Lee MY, Moerner WE. *Optica*, 2016, 3: 659–666
32 Backlund MP, Arbabi A, Petrov PN, Arbabi E, Saurabh S, Faraon A, Moerner WE. *Nat Photon*, 2016, 10: 459–462
33 Contreras-Naranjo JC, Wei Q, Ozcan A. *IEEE J Sel Top, Quantum Electron*, 2016, 22: 392–405
34 Wei Q, Luo W, Chiang S, Kappel T, Mejia C, Tseng D, Chan RYL, Yan E, Qi H, Shabbir F, Ozkan H, Feng S, Ozcan A. *ACS Nano*, 2014, 8: 12725–12733
35 Kühnemund M, Wei Q, Darai E, Wang Y, Hernández-Neuta I, Yang Z, Tseng D, Ahlford A, Mathot L, Sjöblom T, Ozcan A, Nilsson M. *Nat Commun*, 2017, 8: 13913
36 Ma F, Li Y, Tang B, Zhang CY. *Acc Chem Res*, 2016, 49: 1722–1730
37 Ha T, Tinnefeld P. *Annu Rev Phys Chem*, 2012, 63: 595–617
38 Yu H, Shan X, Wang S, Chen H, Tao N. *ACS Nano*, 2014, 8: 3427–3433
39 Dinish US, Song Z, Ho CJH, Balasundaram G, Attia ABE, Lu X, Tang BZ, Liu B, Olivo M. *Adv Funct Mater*, 2015, 25: 2316–2325
40 Neuman KC, Nagy A. *Nat Meth*, 2008, 5: 491–505
41 Shiotari A, Sugimoto Y. *Nat Commun*, 2017, 8: 14313
42 Kim S, Blainey PC, Schroeder CM, Xie XS. *Nat Meth*, 2007, 40: 397–399
43 Footer MJ, Kerssemakers JWJ, Theriot JA, Dogterom M. *Proc Natl Acad Sci USA*, 2007, 104: 2181–2186
44 Bezrukavnikov S, Mashaghi A, van Wijk RJ, Gu C, Yang LJ, Gao YQ, Tans SJ. *Soft Matter*, 2014, 10: 7269–7277
45 Heller I, Laurens N, Vorselen D, Broekmans OD, Biebricher AS, King GA, Brouwer I, Wuite GJL, Peterman EJG. *Optical Tweezers: Methods and Protocols*. New York: Springer New York, 2017. 257–272
46 De Vlaminck I, Dekker C. *Annu Rev Biophys*, 2012, 41: 453–472
47 Sarkar R, Rybenkov VV. *Front Phys*, 2016, 4: 48
48 Kriegel F, Ermann N, Lipfert J. *J Struct Biol*, 2017, 197: 26–36
49 Cluzel P, Lebrun A, Heller C, Lavery R, Viovy JL, Chatenay D, Caron F. *Science*, 1996, 271: 792–794
50 Evans E, Ritchie K, Merkel R. *BioPhys J*, 1995, 68: 2580–2587
51 Chakraborty K, Veetil AT, Jaffrey SR, Krishnan Y. *Annu Rev Biochem*, 2016, 85: 349–373
52 Endo M, Sugiyama H. *Acc Chem Res*, 2014, 47: 1645–1653
53 Gu H. *Sci China Chem*, 2017, 60, doi: 10.1007/s11426-017-9073-6
54 Alonso-Sarduy L, Longo G, Dietler G, Kasas S. *Nano Lett*, 2013, 13: 5679–5684
55 Quigley GJ, Wang AHJ, Ughetto G, van der Marel G, van Boom JH, Rich A. *Proc Natl Acad Sci USA*, 1980, 77: 7204–7208
56 Li M, Liu L, Xiao X, Xi N, Wang Y. *Sci China Mater*, 2017, 60: 269–278
57 Fire A, Xu SQ, Montgomery MK, Kostas SA, Driver SE, Mello CC. *Nature*, 1998, 391: 806–811
58 Timmons L, Fire A. *Nature*, 1998, 395: 854–854
59 Montgomery MK, Xu S, Fire A. *Proc Natl Acad Sci USA*, 1998, 95: 15502–15507
60 Hormeño S, Ibarra B, Carrascosa JL, Valpuesta JM, Moreno-Herrero F, Arias-Gonzalez JR. *BioPhys J*, 2011, 100: 1996–2005
61 Hormeño S, Moreno-Herrero F, Ibarra B, Carrascosa JL, Valpuesta JM, Arias-Gonzalez JR. *BioPhys J*, 2011, 100: 2006–2015
62 Hormeño S, Ibarra B, Valpuesta JM, Carrascosa JL, Ricardo

Arias-Gonzalez J. *Biopolymers*, 2012, 97: 199–208
63 Herrero-Galán E, Fuentes-Perez ME, Carrasco C, Valpuesta JM, Carrascosa JL, Moreno-Herrero F, Arias-Gonzalez JR. *J Am Chem Soc*, 2013, 135: 122–131
64 Pyne A, Thompson R, Leung C, Roy D, Hoogenboom BW. *Small*, 2014, 10: 3257–3261
65 Ares P, Fuentes-Perez ME, Herrero-Galán E, Valpuesta JM, Gil A, Gomez-Herrero J, Moreno-Herrero F. *Nanoscale*, 2016, 8: 11818–11826
66 Schön P. *Methods*, 2016, 103: 25–33
67 Zhang Y, Chen S, Ouyang Z, Hu J, Xiong Q, Li B, Huang Y, Li M, Jin C. *Chin Sci Bull*, 2000, 45: 1365–1368
68 Chan TF, Ha C, Phong A, Cai D, Wan E, Leung L, Kwok PY, Xiao M. *Nucleic Acids Res*, 2006, 34: e113–e113
69 Neupane GP, Dhakal KP, Kim MS, Lee H, Guthold M, Joseph VS, Hong JD, Kim J. *J Biomed Opt*, 2014, 19: 051210
70 Kim N, Kim HJ, Kim Y, Min KS, Kim SK. *Anal Bioanal Chem*, 2016, 408: 6453–6459
71 Sørensen KT, Lopacinska JM, Tommerup N, Silahtaroglu A, Kristensen A, Marie R. *Rev Sci Instrum*, 2015, 86: 063702
72 Rems L, Kawale D, Lee LJ, Boukany PE. *Biomicrofluidics*, 2016, 10: 043403
73 Gross P, Laurens N, Oddershede LB, Bockelmann U, Peterman EJG, Wuite GJL. *Nat Phys*, 2011, 7: 731–736
74 Candelli A, Wuite GJL, Peterman EJG. *Phys Chem Chem Phys*, 2011, 13: 7263–7272
75 Suei S, Raudsepp A, Kent LM, Keen SAJ, Filichev VV, Williams MAK. *Biochem BioPhys Res Commun*, 2015, 466: 226–231
76 Liu S, Chistol G, Bustamante C. *BioPhys J*, 2014, 106: 1844–1858
77 Xu H, Li Q, Wang L, He Y, Shi J, Tang B, Fan C. *Chem Soc Rev*, 2014, 43: 2650–2661
78 Baday M, Cravens A, Hastie A, Kim HJ, Kudeki DE, Kwok PY, Xiao M, Selvin PR. *Nano Lett*, 2012, 12: 3861–3866